APPLIED AND ENVIRONMENTAL MICROBIOLOGY, Feb. 2009, p. 784–791 Vol. 75, No. 3
0099-2240/09/$08.00+0 doi:10.1128/AEM.02481-08

Bioinformatic and Expression Analyses of Genes Mediating Zinc Homeostasis in *Nostoc punctiforme*▽†

Lee Hudek,[1] L. C. Rai,[2] David Freestone,[1] Agnes Michalczyk,[1] Maria Gibson,[1] Y. F. Song,[3] and M. Leigh Ackland[1]*

Centre for Cellular and Molecular Biology, School of Life and Environmental Sciences, Deakin University, Burwood, Victoria 3125, Australia[1]; Molecular Biology Unit, Laboratory of Algal Biology, CAS in Botany, Banaras Hindu University, Varanasi 221005, India[2]; and Key Laboratory of Terrestrial Ecological Processes, Institute of Applied Ecology, Chinese Academy of Sciences, Shenyang, People's Republic of China[3]

Received 29 October 2008/Accepted 4 November 2008

Zinc homeostasis was investigated in *Nostoc punctiforme*. Cell tolerance to Zn^{2+} over 14 days showed that $ZnCl_2$ levels above 22 μM significantly reduced cell viability. After 3 days in 22 μM $ZnCl_2$, ca. 12% of the Zn^{2+} was in an EDTA-resistant component, suggesting an intracellular localization. Zinquin fluorescence was detected within cells exposed to concentrations up to 37 μM relative to 0 μM treatment. Radiolabeled ^{65}Zn showed Zn^{2+} uptake increased over a 3-day period, while efflux occurred more rapidly within a 3-h time period. Four putative genes involved in Zn^{2+} uptake and efflux in *N. punctiforme* were identified: (i) the predicted Co/Zn/Cd cation transporter, putative CDF; (ii) the predicted divalent heavy-metal cation transporter, putative Zip; (iii) the ATPase component and Fe/Zn uptake regulation protein, putative Fur; and (iv) an ABC-type Mn/Zn transport system, putative zinc ZnuC, ZnuABC system component. Quantitative real-time PCR indicated the responsiveness of all four genes to 22 μM $ZnCl_2$ within 3 h, followed by a reduction to below basal levels after 24 h by putative ZIP, ZnuC, and Fur and a reduction to below basal level after 72 h by putative CDF efflux gene. These results demonstrate differential regulation of zinc transporters over time, indicating a role for them in zinc homeostasis in *N. punctiforme*.

Cyanobacteria are photosynthetic prokaryotes, many of which accumulate heavy metals. Consequently, they have attracted interest as a tool for the removal of metals from wastewater. Cyanobacteria, including *Anabaena nodosum* (10), *Nostoc linkia* (12), *Microcystis aeruginosa* (39), and *Synechococcus* sp. strain PCC7942 (16), are able to accumulate the heavy metals cadmium, zinc, copper, and chromium, respectively. Heavy metal accumulation involves an initial rapid, passive adsorption of the metal to components of the cell wall over seconds or minutes, followed by a slower process that results in the sequestration of the metal to an EDTA-resistant compartment, such as the cytoplasm, within hours (for reviews, see references 7 and 29). Cell wall components that have a high affinity for metals account for the bulk of the adsorbed metals (17). In *M. aeruginosa*, metal accumulation was only marginally decreased in cells treated with metabolic inhibitors and in heat-killed cells compared to the total metal uptake (34). Substantial data exist showing sorption of metals in cyanobacteria; however, the capacity of live cells to tolerate or accumulate metals and the molecular mechanisms underlying these processes are relatively unknown. In contrast to many bacterial species, cyanobacteria possess a metallothionein, SmtA, which may store Zn^{2+} and prevent intracellular Zn^{2+} toxicity (8). Polyphosphate granules may sequester intracellular metal ions, including zinc ions (4). These cellular characteristics make cyanobacteria unique organisms in regard to their ability to accumulate metals.

Genomic analysis indicated that *Nostoc punctiforme*, a filamentous cyanobacterium, contains transporters that may function in metal uptake and efflux (3). There are 262 open reading frames (ORFs) of encoding proteins predicted to be involved in transport of small organic and inorganic molecules across the cell membrane, and a further 89 ORFs have been provisionally identified as encoding the ATPase domain of assigned and unassigned membrane-associated ATP-binding cassette (ABC) transport systems (28). In addition, 48 organic carbon and ion transporting permeases not associated with ABC transporters have been identified in *N. punctiforme*. Included in this list are several families of transporters known to facilitate the cellular influx and efflux of zinc (28).

To gain an understanding of the capacity of *N. punctiforme* to regulate Zn^{2+}, we investigated the growth response of *N. punctiforme* to $ZnCl_2$ over a time period of 14 days. Intracellular zinc levels were measured over a period of 3 days, and intracellular zinc in cells was visualized by using Zinquin fluorescent marker. Investigations into physiological Zn^{2+} uptake and efflux indicated that there is a link between zinc uptake and efflux and Zn^{2+} transport gene activity. Four genes involved in Zn^{2+} uptake and efflux in *N. punctiforme* were differentially expressed in response to extracellular Zn^{2+}, demonstrating a role for them in zinc homeostasis.

MATERIALS AND METHODS

Cell culture. *N. punctiforme* PCC73120 cells were a generous donation from Brett Neilan (Cyanobacteria and Astrobiology Research Laboratory, University of New South Wales). Stock cultures of *N. punctiforme* were grown in 500 ml of

* Corresponding author. Mailing address: Deakin University, Burwood Campus, 221 Burwood Highway, Burwood, Victoria 3125, Australia. Phone: 613 925 17036. Fax: 613 925 17048. E-mail: leigha@deakin.edu.au.

† Supplemental material for this article may be found at http://aem.asm.org/.

▽ Published ahead of print on 14 November 2008.

BG11 broth (3) in sterile 2,000-ml conical flasks covered with loose sterile foil. Flasks were placed on a shaker table at 160 rpm in an incubator at 25°C, with 16-h light (cool-white fluorescent light at 70 μmol/m^2/s) and 8-h dark cycling. The medium was changed every 2 weeks. Flasks were only opened in sterile laminar flow cabinets, keeping stocks free of contaminants. Experiments involving $ZnCl_2$ treatments were conducted in 200-ml conical flasks containing 25 ml of culture medium.

Viable cell counts. Prior to counting cells, colonies of cells from each treatment were broken up by syringing (10-ml Terumo syringe, 25G Terumo needle) for 2 min or until cells appeared to be evenly distributed. An aliquot of 10 μl from treatments was mixed with 0.5% trypan blue solution (Sigma-Aldrich, Melbourne, Australia), and viable cell numbers were determined with a hemacytometer based on trypan blue exclusion by healthy cells (5). Numbers of live and dead cells were recorded. Cell viability was measured at intervals of 24 h. This was used to establish effects of $ZnCl_2$ on all treatments.

Zinc treatment. A stock solution of zinc chloride ($ZnCl_2$; Merck, Darmstadt, Germany) at a concentration of 84 mM was prepared. Aliquots of the $ZnCl_2$ stock were added to the BG11 medium for treatments. The pH was adjusted to 7.8 (Hanna Instruments HI8424 microcomputer pH meter). Triplicates of 25-ml cultures containing an initial weight of 150 mg of cells were grown in $ZnCl_2$ concentrations ranging from, 22 to 37 μM over a 14-day period. Controls cells were grown in medium without $ZnCl_2$ for comparison (0 μM).

Speciation and levels of free zinc were analyzed by using MINEQL+ software (version 4.5). The results from MINEQL+ indicated that there was a ~12% reduction in free zinc at pH 7.8 from 22 μM $ZnCl_2$ to ~17.5 μM $ZnCl_2$. This reduction in free zinc is consistent with free zinc reductions at a pH of 7.8 in other studies (40). The results from previous studies have indicated that shifts in pH affect gene expression and that upregulation of some zinc transport genes occurs at a lower pH, whereas other zinc transport genes upregulate at a higher pH, since pH affects free zinc levels (40). In order to prevent shifts in gene regulation through changes in pH, a constant pH was kept across all experiments, providing optimum conditions for cell growth and a nonbiased result for zinc transporter gene expression across treatments.

Quantification of intracellular and extracellular zinc using atomic absorption spectroscopy. Cells were treated for 3 days with 0 μM $ZnCl_2$ (control) or 22 μM $ZnCl_2$; this corresponds to <0.001 or 0.8 ppm of zinc, respectively. Samples taken from each treatment group were divided into two groups, and half were treated with 1 ml of 20 mM EDTA (pH 8.0) for 15 min prior to harvesting (to remove adsorbed zinc), while the remainder were harvested immediately after treatment. Cells were centrifuged for 10 min at 2,500 × *g*, and the supernatant was retained. Media (1.5 ml) and EDTA treatment serum were collected for further analysis. EDTA was also tested for purity, indicating that Zn levels in EDTA were $<10^{-8}$ ppm. Cells (3×10^5) from each treatment were collected and dried in a heating block at 60°C for 8 h. Supernatants and pellets were analyzed for zinc by using flame atomic absorption spectroscopy (AAS).

Fluorescence detection of zinc localization using Zinquin fluorescent label. After exposure to 0, 22, and 37 μM $ZnCl_2$, the cells were harvested and centrifuged for 10 min at 2,500 × *g*, rinsed once in 25 ml of phosphate-buffered saline, and centrifuged again for 10 min at 2,500 × *g*, and the supernatant was then aspirated. Next, 500 μl of 1:10- diluted (1 mg/ml) Zinquin ethyl ester (Biotium, Adelaide, Australia) fluorescent marker was mixed with cell pellets. After incubation at 37°C for 30 min, cells were rinsed in PBS and viewed by using an inverted confocal scanning laser microscope (Leica DM IRE2Mod. no. 0871 with Leica confocal software v2.00Build). The settings used for all images were Ar/HeNe laser at 458 nm (90%), with channel 1 (PMT1) set for detecting Zinquin marker, with a range of 480 to 525 nm (cyan), and channel 2 (PMT2) set for detecting autofluorescence, with a range from 660 to 720 nm (red).

Physiological zinc uptake and efflux. Two sets of 100-mg cell pellets were weighed out for 0-h, 3-h, 1-day, 3-day, and 6-day treatments, in triplicates, for the uptake experiments. Cells were cultured in 1 ml of 22 μM $ZnCl_2$ medium added at time zero to both sets of cells. One set had 0.5 μCi of ^{65}Zn (Oak Ridge National Laboratory, Oak Ridge, TN) added to the 22 μM $ZnCl_2$ medium. Immediately, three samples were taken from both treatments for the 0-h time point. Cells from both treatments were centrifuged at 8,000 × *g* for 2 min. The cells were then rinsed with 1 ml of 20 mM EDTA to remove the adsorbed zinc. Cell pellets containing ^{65}Zn, the medium, and the EDTA rinse were retained, and the counts per minute of ^{65}Zn were obtained (Perkin-Elmer 1480 automatic gamma counter). Nonradiolabeled cells were treated as described for the ^{65}Zn-labeled cells; however, cell pellets were retained, and the total protein was measured (Pierce BCA protein assay kit; Thermo Scientific) (1, 41). This was repeated for the 3-h and 1-, 3-, and 6-day treatments. The data was recorded in Microsoft Excel as counts per minute in cell pellets and protein concentrations, and then the picomoles of Zn/microgram of protein values were calculated (1). For efflux experiments, cells were incubated in 22 μM $ZnCl_2$ containing 0.5 μCi of ^{65}Zn/ml for 24 h. The ^{65}Zn was removed, and the cells were incubated in 22 μM $ZnCl_2$ with no ^{65}Zn for 0 and 3 h and 1, 3, and 6 days. Pellets were obtained for radioactive analysis as described for the uptake experiments.

Identification of zinc uptake and efflux genes. To identify zinc transporter genes present in *N. punctiforme* protein sequences encoding putative zinc transporters from other prokaryotic organisms, including *Escherichia coli*, *Synechococcus* species, *Synechocystis* species, and *Nostoc* species were used as bait for Basic Local Alignment Search Tool (BLAST) searching. BLAST searches were restricted to the known *N. punctiforme* genomic sequence (http://img.jgi.doe.gov/cgi-bin/pub/main.cgi).

Multiple sequence alignments were produced for *N. punctiforme*, *Nostoc* sp. strain PCC7120, *Synechococcus* sp. strain JA-3-3Ab, *Synechocystis* sp. strain 6803, *E. coli* F11, and *Arabidopsis thaliana* Columbia using CLUSTAL X (v1.83 for Windows), since the genomes of these species have been fully sequenced (23, 43, 44). The percent homology for the aligned sequences was determined by using BOXSHADE (v3.21 for DOS) (25). The predicted protein structures for the identified Zn^{2+} uptake and efflux genes in *N. punctiforme* were determined by using the shareware program for the Transmembrane Hidden Markov Model (TMHMM; http://www.cbs.dtu.dk/services/TMHMM-2.0/ [K. Hoffman, Bioinformatics Group, ISREC, Epalinges/Lausanne, Switzerland]).

RNA isolation, purification, and synthesis of cDNA by reverse transcriptase from *N. punctiforme*. RNA extractions were carried out by using Qiagen RNeasy plant minikit, including all listed buffers (Corbett Life Science, Victoria, Australia). Kit methods were adapted as follows. Cells (150 mg) were crushed by using liquid nitrogen in a mortar and pestle, and 450 μl of RLT buffer, containing 1% β-mercaptoethanol was added, along with 1 μl of RNase inhibitor. The sample was then pipetted into a shredder column and spun at full speed for 2 min. The supernatant was collected, another 450 μl of RLT buffer containing 1% β-mercaptoethanol was added, and the process was repeated. The supernatant was collected, and 0.5 μl of 100% ethanol was added; the solution was then mixed and pipetted directly onto the binding column and spun for 15 s at 8,000 × *g*. The flowthrough was discarded, and 350 μl of RW1 buffer was added directly to the column and spun through at 8,000 × *g* for 15 s. The flowthrough was discarded, and 140 μl of the RDD buffer with 20 μl of DNase I stock was added directly to the binding column, followed by incubation at 25°C for 20 min, before 350 μl of RW1 was added directly to the binding column, and the sample was then spun at 8,000 × *g* for 15 s. The flowthrough was discarded, and this step repeated with 70 μl of the RDD buffer, 10 μl of DNase I stock, and 700 μl of RW1 buffer.

The remainder of the RNA extraction protocol was carried out as described in the kit, and RNA was eluted off the column by using 30 μl of RNase-free H_2O. Immediately after elution, 1 μl of RNase inhibitor was added to prevent degradation. RNA was then treated using an Ambion DNA-free kit according to the manufacturer's protocol (Ambion, Melbourne, Australia) with 1 μl of RNase inhibitor added to the RNA after the Ambion DNA-free treatment. RNA concentrations were determined by using a Beckman Coulter DU530 Life Science UV/Vis spectrophotometer. RNA electrophoresis through agarose gels containing formaldehyde, using 20 μg of RNA from all RNA preparations, was carried out, confirming template quality. Total RNA (10 μg) concentrations were determined by using a spectrophotometer, and then RNA was reverse transcribed using Stratagene Stratascript reverse transcriptase as described by the manufacturer's protocol (Promega, Australia).

Gene expression analysis using qRT-PCR. Quantitative real-time reverse transcription-PCR (qRT-PCR) was used to identify putative Zn^{2+} transport genes in *N. punctiforme* whose expression was regulated by exposure to Zn^{2+}. Primers were designed to selected regions of sequences obtained through BLAST searching, using the computer program Primer Express (Primer Express v2.0 for Windows 2000; Applied Biosystems) (Table 1). Primer Express analyses focus on primer secondary structures and dimers, allowing optimum primers to be designed. Primer binding efficiencies were established through using 1, 2, 4, and 8 μg of template cDNA/ml as a control and then comparing the cycle time of amplification against a log scale. Primer binding efficiencies were all <0.1. Using PCR with primer sets containing no template, visualized on agarose gels, primer dimers were assessed, indicating no dimers in the primers used. The primers were purchased from Sigma-Aldrich (Melbourne, Australia). Real-time qRT-PCR was performed using 1× SYBR green master mix (Applied Biosystems, Melbourne, Australia) and 20 ng of cDNA template determined by using a spectrophotometer, and 0.3 μM concentrations of forward and reverse primer were used as described by the manufacturer's protocol. qRT-PCR analyses were conducted by using Applied Biosystems 7500 real-time PCR system and data produced through Biosystems 7500 SDS software.

Statistical methods. Statistical methods used were based on normally distributed data. The data sets were all firstly produced in Microsoft Excel. Bar graphs

TABLE 1. Primers for qRT-PCR[a]

Primer	Primer sequence (5′–3′)
16S RNA F	AGCAGCCGCGGTAATACG
16S RNA R	CGCTTTACGCCCAATCATTC
COG0053 F	AGCAATTGTTACTATTGCCTTGAAGTTT
COG0053 R	GCCCACAGTGCCACCAA
COG0428 F	GCAAAGCACCGCAAACG
COG0428 R	CCCACTCCCACTATTTTCCTCTT
COG0735 F	CCCCAGCGCGAAACAAT
COG0735 R	TGATCCCTTCACCATCAGTTTCT
COG1121 F	ATCGGCAGCAGTAGGAGAAGC
COG1121 R	AAGTTGGCCACCGCTAAGAGT

[a] Primers are listed in sets of forward and reverse (F and R). 16S RNA are genomic controls. COG0053, COG0428, COG0735, and COG1121 are the product names of the genes from which the primers were derived. The accession numbers for the sequences used were ZP_00110704 (COG0053), ZP_00110916 (COG0428), ZP_00108619 (COG0735), ZP_00109802 (COG1121), and AF027655 (16S RNA).

were produced for viability tests, flame AAS, physiological Zn uptake and efflux, and qRT-PCR data using Microsoft Excel. The statistical computer program SPSS (v12.0.1 for Windows) was used for all statistical analysis. Probability plots (P-P plots) were produced for all data sets to test for normal distribution. Statistical tests used were a one-way analysis of variance and Tukey's honest significant difference test for the growth curve data, AAS data, and qRT-PCR data. All statistical analysis was tested against a probability value (P) of < 0.05.

RESULTS

Cell viability in $ZnCl_2$. To establish concentrations of $ZnCl_2$ that *N. punctiforme* can tolerate, cells were cultured in zinc concentrations ranging from 0 to 37 μM for 14 days. Viable cell numbers for treatments were detected by using trypan blue exclusion tests (40). Concentrations of $ZnCl_2$ exceeding 22 μM caused a significant ($P < 0.05$) decline in the numbers of viable cells present after 14 days. In contrast, cells treated with 22 μM showed no significant decrease in cell number compared to control cells (Fig. 1).

Quantification of intracellular and extracellular zinc using atomic absorption spectroscopy. Quantification of the EDTA-resistant and EDTA-sensitive Zn^{2+} levels were carried out using flame AAS. These results showed that significantly more Zn^{2+} was in the EDTA-sensitive fraction (55 ng/10^6 cells) compared to the EDTA-resistant fraction (8 ng/10^6 cells) ($P < 0.05$). In cultures treated with 22 μM $ZnCl_2$ for 3 days, there was significantly less Zn^{2+} in the EDTA-resistant fraction compared to the EDTA-sensitive fraction, where the ratios of

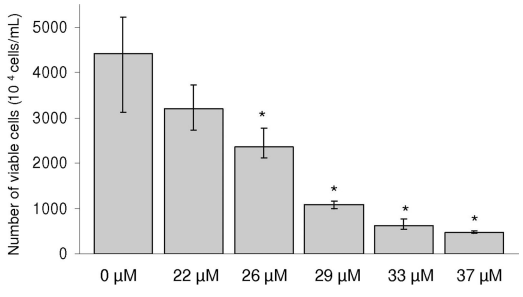

FIG. 1. Trypan blue exclusion testing for *N. punctiforme* cells treated with various $ZnCl_2$ concentrations, beginning at 22 μM and increasing to 37.0 μM, indicate that after 14 days exposure to ≥26 μM $ZnCl_2$ the samples had significantly fewer cells ($P < 0.05$) compared to control cells, as denoted by an asterisk (*).

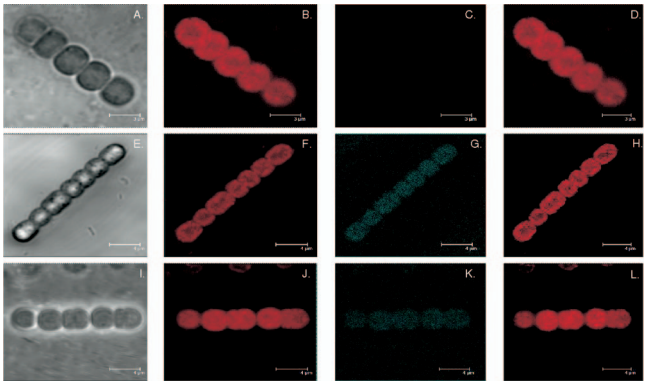

FIG. 2. Fluorescence microscopy images showing Zinquin marker within cells exposed to $ZnCl_2$. The images show the control cells with 0 μM $ZnCl_2$ treatment (A to D) and treatments of 22 and 37 μM $ZnCl_2$ (E to H and I to L, respectively). Phase-contrast images indicate cell morphology (A, E, and I). Autofluorescence is shown in red (B, F, and J). Zinquin fluorescent marker for zinc localization is shown in cyan (C, G, and K). Overlay of the autofluorescence and Zinquin images indicates the localization of free zinc (D, H, and L).

Zn^{2+} in the EDTA-sensitive fraction to the EDTA-resistant fraction were 6.8.

Fluorescence detection of zinc localization using Zinquin. Accumulation of zinc by *N. punctiforme* was further investigated by using fluorescence detection microscopy. Cells were grown in 0, 22, and 37 μM $ZnCl_2$ and treated with Zinquin fluorescent marker. Phase-contrast images of cells indicate cell morphology (Fig. 2A, E, and I). Live cells are indicated by autofluorescence (red) (Fig. 2B, F, and J). Zinquin fluorescence (cyan) is relative to intracellular zinc levels (Fig. 2C, G, and K). The overlay of Zinquin and autofluorescence indicates no specific site of cellular localization, being uniformly stained (Fig. 2G, K, H, and L). In cells treated at 0 μM, little Zinquin fluorescence was detected in live cells (Fig. 2C). At 22 and 37 μM $ZnCl_2$ there was noticeably more Zinquin fluorescence than with the 0 μM treatment (Fig. 2G, K, and C).

Physiological zinc uptake and efflux. Physiological zinc uptake and efflux using radiolabeled zinc (^{65}Zn) supports the findings from AAS and fluorescence microscopy, confirming that zinc was taken up intracellularly (Fig. 3A). Uptake studies indicate that zinc uptake increased significantly from 0 h to 3 days (Fig. 3A). At day 6, zinc uptake was similar to day 3. Efflux studies indicated a reduction in zinc between the 0 and 3 h, with no change up to day 6 (Fig. 3B).

Predicted structure, transmembrane domains, and intracellular localization of zinc uptake and efflux genes. Four putative zinc transport genes were identified: (i) predicted Co^{2+}/Zn^{2+}/Cd^{2+} cation transporter, putative CDF (COG0053); (ii) predicted divalent heavy-metal cation transporter, putative ZIP (COG0428); (iii) ATPase component and Fe^{2+}/Zn^{2+} uptake regulation protein, putative Fur (COG0735); and (iv) ABC-type Mn^{2+}/Zn^{2+} transport system, putative zinc ZnuC (COG1121). The transmembrane domains of putative ZIP and CDF were further analyzed to confirm transporter family classification (see Table S1 in the supplemental material).

Alignment of the putative *N. punctiforme* zinc uptake and efflux genes with other established and putative zinc transporter genes, in other species, indicates homologous amino

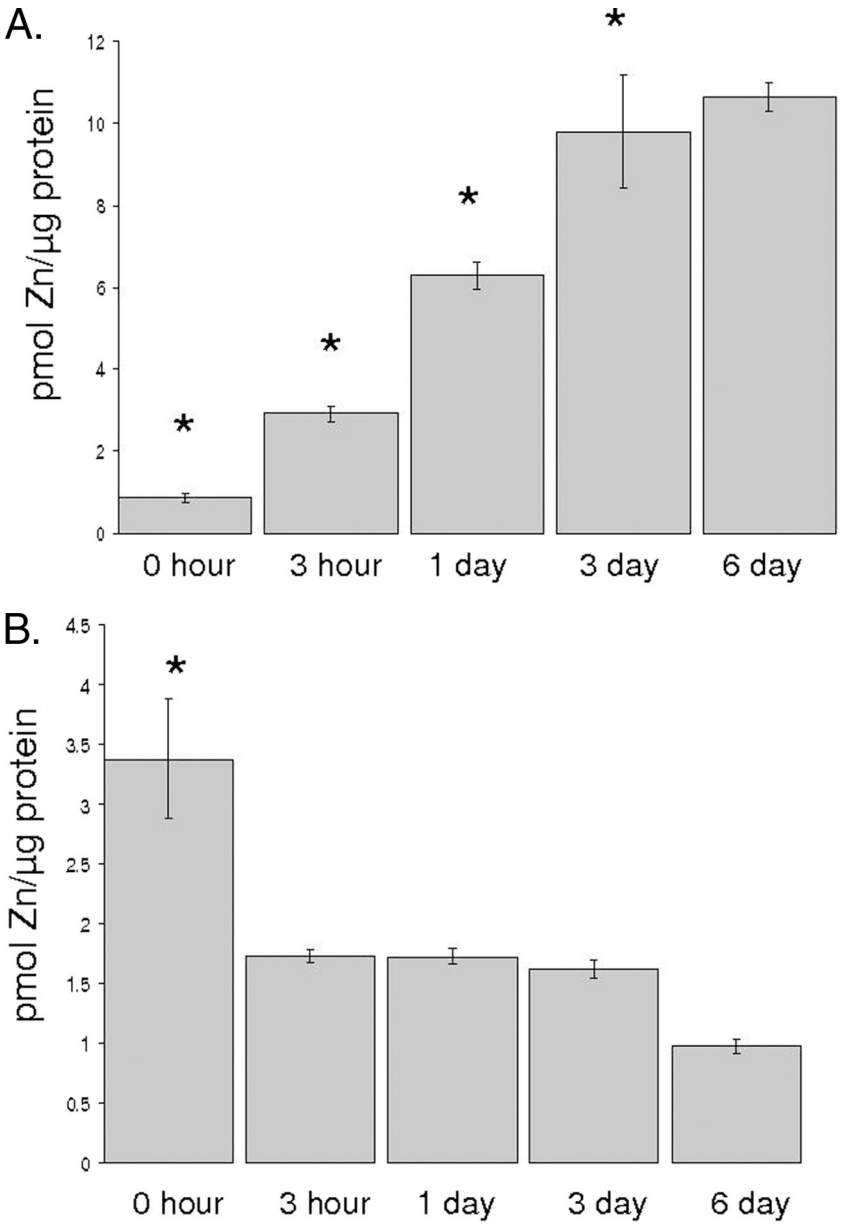

FIG. 3. Physiological zinc uptake and efflux. (A) Intracellular zinc levels increased after 0- and 3-h and 1-, 3-, and 6-day treatments. *P* values are all <0.001 compared to the 6-day values, except for the 3-day treatment ($P = 0.528$). (B) Intracellular zinc decreased significantly compared to 0-h treatment; the *P* values are 0.016, 0.016, 0.009, and <0.001, respectively, compared to the 0-h treatment.

acid residues. The name of the aligned species and the corresponding names and transporter type were tabulated (Table 2). The percent homologies for alignments of *N. punctiforme* zinc uptake and efflux genes with the zinc uptake and efflux genes of other species were determined by using BOXSHADE (v3.21; K. Hoffman, Bioinformatics Group).

Multiple sequence alignments for the putative CDF (COG0053) in *N. punctiforme*, indicate that the predicted (PRED) gene from *Synechococcus* (JA-3-3Ab) was the most similar to the putative CDF, with 71.7% similarity. The least similar gene was *A. thaliana* MTPC1, which had 26.6% similarity.

Multiple sequence alignments for the putative ZIP (COG0428) in *N. punctiforme* indicate that the ZIP gene from *Synechococcus* (JA-3-3Ab) was the most similar to the putative ZIP (39% similarity) and showed the most divergence from *A. thaliana* ZIP (34.4% similarity).

Multiple sequence alignments for the putative Fur illustrate that the Fur in *Nostoc* sp. strain PCC7120 is the most similar gene to *N. punctiforme*, with a very high similarity percentage of 98%. The lowest sequence similarity was seen in comparison to *A. thaliana* ATL1G (14.6% similarity).

Multiple sequence alignments for the putative ZnuC (COG1121) illustrated that the ABC transporter in *Nostoc* sp. strain PCC7120 was the most similar gene to COG1121 (86.1% similarity). *N. punctiforme* COG1121 had least similarity to *A. thaliana*, with 11.3% similarity to *N. punctiforme* COG1121.

TABLE 2. Genes used for multiple sequence alignments[a]

Locus tag	Gene used for sequence alignments					
	N. punctiforme	*Nostoc* sp. strain PCC7120	*Synechococcus* sp. strain JA-3-3Ab	*Synechocystis* sp. strain 6803	*E. coli*	*A. thaliana*
COG0053	CDF	CECS	PRED	HYP	CDF	MTPC1
COG0428	ZIP	HYP	ZIP	cAMP	ZIP	ZIP
COG1121	ZnuC	ATP	MZT	ABC	ZnuC	ABC
COG0735	Fur	Fur	Fur	Fur	Fur	ATL1G

[a] The gene product names for the *N. punctiforme* zinc uptake or efflux genes are in the leftmost column. Species used for alignments are listed across the top, along with abbreviated names in sequence legends. PRED are predicted genes, and HYP are hypothetical genes. Genes were retrieved as top results from BLAST searches using both the http.img.jgi.doe.gov and the http.www.ncbi.nlm.nih.gov databases. The accession numbers for the *N. punctiforme* sequences used were ZP_00110704 (COG0053), ZP_00110916 (COG0428), ZP_00108619 (COG0735), ZP_00109802 (COG1121), and AF027655 (16S RNA). The accession numbers for the *Nostoc* sp. strain PCC7120 sequences used were NP_486940 (COG0053), NP_484517 (COG0428), NP_485731 (COG0735), and NP_484875 (COG1121). The accession numbers for the *Synechococcus* sp. strain JA3-3Ab sequences used were YP_473967 (COG0053), YP_475281 (COG0428), YP_473526 (COG0735), and YP_440431 (COG1121). The accession numbers for the *Synechocystis* sp. strain 6803 sequences used were NP_441464 (COG0053), NP_443044 (COG0428), NP_443047 (COG0735), and NP_440431 (COG1121). The accession numbers for the *E. coli* sequences used were ZP_0072428 (COG0053), NP_755660 (COG0428), NP_286398 (COG0735), and NP_308807 (COG1121). The accession numbers for the *A. thaliana* sequences used were NP_850480 (COG0053), NP_566669 (COG0428), NP_t174614 (COG0735), and AAM61469 (COG1121).

Gene regulation in response to $ZnCl_2$ treatment. Cells were grown in Zn^{2+}-free culture medium for a week. Cells were then treated with 0 and 22 μM concentrations of $ZnCl_2$ for 3, 24, and 72 h. Changes in mRNA expression were measured, establishing the responsiveness of the Zn^{2+} transporter genes to Zn^{2+}. At 3 h the putative ZIP (COG0428) transporter showed a 10-fold increase in gene expression compared to the control (Fig. 4A). After 24 h, the expression levels of the ZIP gene had reduced to the basal levels, and by 72 h ZIP was significantly downregulated below that of the baseline level (Fig. 4A). (The significances of the differences in mRNA expression between treatments were $P < 0.001$ [between the 3- and 24-h treatments], $P < 0.001$ [between the 3- and 72-h treatments], and $P = 0.048$ [between the 24- and 72-h treatments].)

Putative ZnuC uptake component (COG1121) showed a

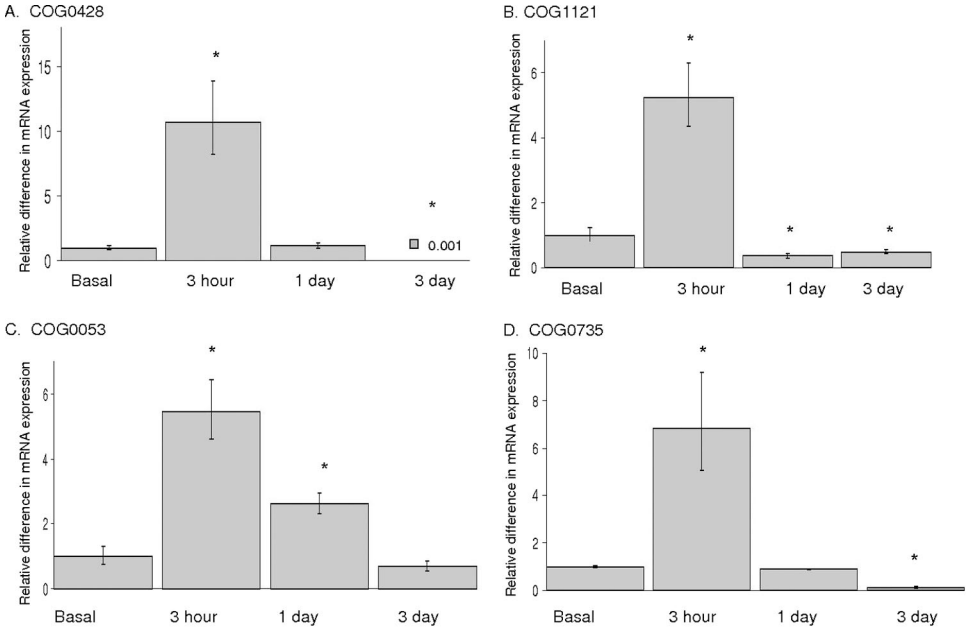

FIG. 4. Relative mRNA expression levels for the putative CDF (COG0053), ZIP (COG0428), ZnuC (COG1121), and Fur (COG0735) genes in response to 22 and 37 μM $ZnCl_2$ at 3, 24, and 72 h. Real-time qRT-PCR was used to detect differences in expression of the putative zinc transporter genes. Significant values ($P < 0.05$) for the 3-, 24-, and 72-h treatments compared to basal levels are denoted by an asterisk (*). A. After a 3-h exposure COG0428 was significantly ($P < 0.05$) upregulated. After a 24-h exposure mRNA expression reverted back to basal levels. After a 72-h exposure there was a further downregulation from a 24-h exposure and a significant ($P < 0.05$) reduction in gene expression below the basal level. (B) After a 3-h exposure COG1121 was significantly ($P < 0.05$) upregulated. After a 24-h exposure there was a significant ($P < 0.05$) downregulation to below basal levels. After a 72-h exposure COG1121 remained significantly downregulated compared to the basal level. (C) After 3-h exposure COG0053 was significantly ($P < 0.05$) upregulated. After 24 h there was a reduction from the 3-h expression level and still a significant ($P < 0.05$) upregulation from basal levels. After a 72-h exposure there was a further downregulation from a 24-h exposure with gene expression being equal to the basal level. (D) After a 3-h exposure COG0735 was significantly ($P < 0.05$) upregulated. After 24 h there was a downregulation of COG0735 to basal levels. After a 72-h exposure there was a further downregulation from the 24-h exposure and a significant ($P < 0.05$) reduction in gene expression below the basal level.

fivefold increase in mRNA expression in the presence of Zn^{2+} compared to the basal level (Fig. 4B). After 24 h of exposure to Zn^{2+}, the putative ZnuC uptake domain showed a 10-fold decrease to levels significantly below that of the baseline. There was no significant difference in expression between 24 and 72 h. (The significances of the differences in mRNA expression between treatments were $P = 0.002$ [between 3- and 24-h treatments], $P = 0.003$ [between 3- and 72-h treatments], and $P = 0.924$ [between 24- and 72-h treatments].)

Putative CDF (COG0053) shows that after 3 h of exposure to $ZnCl_2$ there is a significant fourfold increase in mRNA expression compared to the basal levels (Fig. 4C). After 24 h, expression levels were reduced twofold, although this was still well above basal levels, and by 72 h there was a further threefold reduction in mRNA expression to a level similar to that of the basal (Fig. 4C). (The significances of the differences in mRNA expression between treatments were $P = 0.027$ [between 3- and 24-h treatments], $P = 0.013$ [between 3- and 72-h treatments], and $P = 0.026$ [between 24- and 72-h treatments].)

Putative Fur (COG0735) showed that after 3 h of exposure to $ZnCl_2$ there was a sixfold increase in mRNA expression compared to the basal level (Fig. 4D). At 24 h there was a significant downregulation to a level similar to that of the basal level (Fig. 4D). By 72 h there was a further significant 10-fold reduction in mRNA expression. (The significances of the differences in mRNA expression between treatments were $P = 0.002$, [between 3- and 24-h treatments], $P = 0.001$ [between 3- and 72-h treatments], and $P = 0.237$ [between 24- and 72-h treatments].)

DISCUSSION

Cyanobacteria, including *Nostoc*, have received considerable attention for use as biosorbents to remove heavy metals from contaminated water (12, 14, 24, 34). Metal sorption by different cyanobacterial species ranges greatly (see reference 29 for a review), with sorption as high as 999 mg g^{-1} reported in *Microcystis* sp. (39). The capacity to sorb high concentrations of heavy metals has been attributed to various components of cyanobacteria, in particular polysaccharides of the cell wall (17). Previous studies have shown that sorption of heavy metals by *M. aeruginosa* was not affected by treatment with metabolic inhibitors, low temperatures, and formaldehyde treatment (34), suggesting that the intracellular sequestration of Zn^{2+} was negligible compared to the total Zn^{2+} associated with the cells. We found that in *N. punctiforme* exposed to the nontoxic level of 22 μM, which is significantly less than most other studies, the amount of adsorbed Zn^{2+} (indicated by EDTA-sensitive Zn^{2+} fraction) was 6.8 times that of the EDTA-resistant Zn^{2+} after 3 days.

Considerably less information is available in relation to the longer-term effects of heavy metal treatment and the capacity of cyanobacteria to actively accumulate, retain and efflux heavy metals, since previous studies have focused on short exposures, commonly 1 h (24), 2 h (45), and 6 h (34). The present study shows that *N. punctiforme* can tolerate a maximum $ZnCl_2$ concentration of 22 μM over a 14-day period and that cell numbers were significantly reduced in $ZnCl_2$ treatments of >22 μM. This is not a high threshold compared to zinc concentrations in contaminated waters, which can exceed 500 mg $liter^{-1}$ (2, 13, 46). Zinquin ethyl ester, a membrane-permeable, UV-excitable, blue fluorescent zinc indicator that is hydrolyzed into Zinquin free acid once entering cells, provides a relative estimate of free intracellular Zn^{2+} levels (47), and Zinquin analyses indicated that Zn^{2+} was internalized in both living and dead cells. Zinquin staining of *N. punctiforme* showed that dead cells, identified by the lack of autofluorescence, accumulated more Zn^{2+} than live cells. This suggests that live cells are able to actively exclude Zn^{2+} to prevent intracellular toxicity. This is also supported by data showing that 14% of the Zn^{2+} was internalized relative to the adsorbed or bound Zn^{2+}. The capacity of *N. punctiforme* to regulate intracellular Zn^{2+} was shown by the radiolabeled ^{65}Zn studies, where Zn^{2+} influx increased over a period of 3 days and then stabilized. In contrast efflux from preloaded cells occurred more rapidly in the first 3 h and then remained unchanged for 6 days.

Detoxification of intracellular metals, including zinc, has been found to occur through a variety of different processes. These processes encompass enzymatic reduction or oxidation to a less-toxic form, methylation and diffusion of the methyl metal through the plasma membrane, and complexation by proteins (including metallothioniens) (32, 37). Polyphosphate granules have also been described as having a broad substrate range, sequestering an array of excess intracellular metal ions, including zinc ions (4). Active uptake and efflux systems and their transcriptional regulators have been identified as playing a key role in metal detoxification in an array of organisms (37). In the present study, we identified the presence of zinc influx and efflux systems, suggesting the involvement of zinc transporter genes in homeostasis. We focused here on describing putative genes likely to be involved in active uptake and efflux, as well as transcriptional regulation of metal uptake and efflux systems, in the cyanobacterium *N. punctiforme*. This provides insight into cyanobacterial gene expression responses to zinc treatments.

To identify putative genes that may be involved in zinc homeostasis, BLAST searches were carried out using bait sequences from known families of Zn^{2+} transporters in other prokaryote organisms. These products were then tested for responsiveness to Zn^{2+}. On the basis of sequence homology between *N. punctiforme*, other cyanobacterial species, *A. thaliana*, and *E. coli* genes, four genes involved in zinc uptake and efflux in *N. punctiforme* were identified.

The predicted Co/Zn/Cd cation transporter, putative CDF (COG0053) possessed six transmembrane domains with C and N termini located in the cytoplasm (see Table S1 in the supplemental material). This is consistent with other members of the CDF transporters belonging to the SLC30 family that typically contain six transmembrane domains. Members of the SLC30 typically contain conserved histidine regions in the intracellular loop of the protein between transmembrane 4 and 5 (36). These are postulated to facilitate Zn^{2+} binding (6). Consistent with this observation, we found a total of nine histidine residues, seven of which were conserved. Two of these were located between transmembranes 4 and 5. CDF transporters are postulated to be involved exclusively in transport of Zn^{2+} into intracellular vesicles or out of the cell across the plasma membrane (33). CDF proteins found in bacteria are involved in resistance to Zn^{2+} (31). Few studies have been carried out on the function of these proteins. ZitB in *E. coli* is induced by

Zn^{2+}, and overexpression of this gene reduced the accumulation of ^{65}Zn, suggesting that it mediated the efflux of Zn^{2+} (18). The CzcD protein of *Bacillus subtilis* is a CDF protein whose levels were induced following exposure to Zn^{2+} (20). Since cyanobacteria do not possess intracellular vesicles, it is most likely that COG0053 mediates efflux of Zn^{2+} from the cytoplasm of *N. punctiforme* to the periplasm. Our data are consistent with studies in bacteria where, after 3 h of exposure to $ZnCl_2$, *N. punctiforme* cells showed a fourfold upregulation of COG0053. By 24 h the mRNA levels were reduced by another 50% but remained significantly higher than basal levels, possibly indicating the need to efflux Zn^{2+} to prevent intracellular toxicity in the presence of extracellular zinc. At the 72-h time point, the mRNA levels were still detectable and similar to basal levels.

The putative ZIP (COG0428) protein was identified by TMHMM software as having seven transmembrane domains with the N terminus in the periplasm and the C terminus in the cytoplasm (see Table S1 in the supplemental material). This structure is similar to that of a ZIP or SLC39 family; however, ZIP genes characteristically have eight transmembrane domains in eukaryotes (11). This suggests that COG0428 may be different in cyanobacteria, in that both N and C termini reside in the periplasm. Members of the ZIP family have not been previously studied in cyanobacteria. In *E. coli*, ZupT was the first characterized bacterial member of the ZIP family, and its role in Zn^{2+} uptake was demonstrated by the reduced uptake of ^{65}Zn in *E. coli* strains from which this gene was deleted (18). The structure of COG0428 is consistent with other members of the ZIP family that typically have a long cytoplasmic loop between transmembrane domains 3 and 4, referred to as a variable region since there is little conservation among family members (19). One feature of this region is the presence of many histidine residues that may be potential membrane-binding sites (15). Putative ZIP (COG0428) protein contained three histidine residues located between transmembrane domains 3 and 4, between transmembrane domains 5 and 6, and within transmembrane domain 7. In contrast to plant ZIP proteins, however, COG0428 had only one histidine between transmembrane domains 3 and 4. After 3 h of exposure to $ZnCl_2$, COG0053 was upregulated by 10-fold, and by 24 h the mRNA levels were reduced to a basal rate. After 72 h of exposure, mRNA was almost undetectable. The initial relatively large increase in expression of COG0428 may be due to the need to acquire Zn^{2+} following Zn^{2+}-deficient conditions prior to the addition of Zn^2. Once optimum levels of Zn^{2+} were attained after 24 h, homeostatic mechanisms to prevent further Zn^{2+} uptake may account for the reduced mRNA levels.

The putative ZnuC (COG1121) protein is a component of the Znu Zn^{2+} uptake system that consists of ZnuA, a periplasmic binding protein; ZnuB, a membrane permease; and ZnuC, a soluble ATPase located within the cytoplasm (21). In *E. coli*, this is an ATP-dependent, high-affinity uptake system that is repressed in the presence of 10 μM Zn^{2+} through activation of a zinc uptake regulator (Zur) (35, 48). The putative ZnuC (COG1121) was most similar to the ZnuC in *E. coli* and the ABC transporter in *Synechocystis*, which forms a complex with ZnuA and ZnuB. Upon exposure to Zn^{2+}, ZnuC levels increased by fivefold at 3 h and by 24 and 72 h had dropped below that of the basal level. The initial increase in expression of COG1121 may reflect the need for increasing cellular Zn^{2+} levels, since cells were Zn^{2+} deficient prior to exposure to Zn^{2+}. Once optimum levels of intracellular Zn^{2+} were attained, regulatory mechanisms to prevent excess accumulation of Zn^{2+} may account for the reduction in COG1121 mRNA levels. It is not clear why maximum expression of both ZnuC and Fur was detected at 3 h, since Fur is a repressor and would be expected to inhibit ZnuC. It is possible that other regulators, e.g., SmtB/ArsR, may regulate the expression of the zinc transporter genes (27).

The ferric uptake regulator, *Fur*, encodes repressors that control the transport of Fe^{2+}. The Fur protein binds Fe^{2+} when intracellular iron levels become elevated (22). The coordination of Fe^{2+} to a Fur monomer enables the dimeric Fur protein to bind to a 19-bp DNA sequence called a Fur box within the promoter of the regulated genes (26). Fur proteins contain a cluster of histidine residues around position 90 that may be involved in Fe^{2+} binding (35). The putative Fur (COG0735) in *N. punctiforme* had very high similarity to Fur in *Nostoc* species (PCC7120) and in *Synechococcus* and *Synechocystis*. Interestingly, COG0735 possessed no histidines around position 90, but histidine residues were found at positions 59, 69, 77, 121, and 123 and also at position 133, where there was a sequence of five histidines. A similar placement of five histidine residues is seen in a number of *Bacillus* species, which might provide evidence that the putative Fur (COG0053) in *N. punctiforme* maybe a Zur gene, which is a member of the Fur family. In various bacteria, Zur, a zinc-specific regulator of the Fur family, regulates genes for zinc transport to maintain homeostasis, through binding to ZnuA (42). COG0735 was responsive to Zn^{2+}, since mRNA levels were increased by sevenfold within 3 h of Zn^{2+} treatment. By 24 h the mRNA levels were reduced to below baseline and further reduced after 72 h. This indicates that in *N. punctiforme* Fur is regulated by Zn^{2+}, which is consistent with studies of other organisms, including *Bacillus subtilis* (9), *Pseudomonas aeruginosa*, (38), and *E. coli* (30). Although *N. punctiforme* contains a Zn^{2+}-responsive *Fur* gene, it is not clear whether the Fur protein regulates ZnuABC. *Pasteurellaceae*, which have ZnuABC, have no Zur (21) but have Fur, which might regulate Zn^{2+} uptake by ZnuABC (38).

In summary, *N. punctiforme* showed long-term sensitivity to Zn^{2+}, where concentrations above 22 μM were toxic. In cells exposed to nontoxic levels of Zn^{2+} (22 μM), the accumulation of zinc was accompanied by changes in expression of a Fe^{2+} regulatory gene (*Fur*), two Zn^{2+} uptake genes (one belonging to the SLC39 family of Zn importers and the other a member of the ABC transporter family), and finally one efflux gene belonging to the SLC30 family. The expression of these four genes, together with the identification of cellular zinc influx and efflux processes, indicates that they may play a key role in zinc homeostasis in *N. punctiforme*.

ACKNOWLEDGMENTS

This study was supported by funding from the International Science Linkage Programme, Australia-China Special Fund for Scientific and Technological Cooperation.

We are grateful to Matt Beasley, Ben R. Kiefel (Alchemy Biosciences), and Peter Beech for technical assistance and helpful discussions.

REFERENCES

1. **Ackland, M. L., and H. J. McArdle.** 1996. Cation-dependent uptake of zinc in human fibroblasts. Biometals **9:**29–37.
2. **Al-Hiyaly, S. A. K., T. McNeilly, and A. D. Bradshaw.** 1990. The effect of zinc contamination from electricity pylons. contrasting patterns of evolution in five grass species. New Phytologist **114:**183–190.
3. **Anderson, D. C., E. L. Campbell, and J. C. Meeks.** 2006. A soluble 3D LC/MS/MS proteome of the filamentous cyanobacterium *Nostoc punctiforme*. J. Proteome Res. **5:**3096–3104.
4. **Andrade, L., C. N. Keim, M. Farina, and W. C. Pfeiffer.** 2004. Zinc detoxification by a cyanobacterium from a metal contaminated bay in Brazil. Braz. Arch. Biol. Technol. **47:**147–152.
5. **Asayama, M., S. Imamura, S. Yoshihara, A. Miyazaki, N. Yoshida, T. Sazuka, T. Kaneko, O. Ohara, S. Tabata, T. Osanai, K. Tanaka, H. Takahashi, and M. Shirai.** 2004. SigC, the group 2 sigma factor of RNA polymerase, contributes to the late-stage gene expression and nitrogen promoter recognition in the cyanobacterium *Synechocystis* sp. strain PCC 6803. Biosci. Biotechnol. Biochem. **68:**477–487.
6. **Balesaria, S., and C. Hogstrand.** 2006. Identification, cloning and characterization of a plasma membrane zinc efflux transporter, TrZnT-1, from fugu pufferfish (*Takifugu rubripes*). Biochem. J. **394:**485–493.
7. **Baptista, M. S., and T. M. Vasconcelos.** 2006. Cyanobacteria metal interactions: requirements, toxicity, and ecological implications. Crit. Rev. Microbiol. **32:**127–137.
8. **Blindauer, C. A., M. D. Harrison, A. K. Robinson, J. A. Parkinson, B. P. W., P. J. Sadler, and N. J. Robinson.** 2002. Multiple bacteria encode metallothioneins and SmtA-like zinc fingers. Mol. Microbiol. **45:**1421–1432.
9. **Bsat, N., and J. D. Helmann.** 1999. Interaction of *Bacillus subtilis* Fur (ferric uptake repressor) with the *dhb* operator in vitro and in vivo. J. Bacteriol. **181:**4299–4307.
10. **Chong, K. H., and B. Volesky.** 1996. Metal biosorption equilibria in a ternary system. Biotechnol. Bioeng. **49:**629–638.
11. **Eide, D. J.** 2006. Zinc transporters and the cellular trafficking of zinc. Biochim. Biophys. Acta **1763:**711–722.
12. **El-Enany, A. E., and A. A. Issa.** 2000. Cyanobacteria as a biosorbent of heavy metals in sewage water. Environ. Toxicol. Pharmacol. **8:**95–101.
13. **El Khalil, H., O. El Hamiani, G. Bitton, N. Ouazzani, and A. Boularbah.** 2007. Heavy metal contamination from mining sites in South Morocco: monitoring metal content and toxicity of soil runoff and groundwater. Environ. Monit. Assess. **136:**147–160.
14. **El-Sheekh, M. M., W. A. El-Shouny, M. E. H. Osman, and E. W. E. El-Gammal.** 2005. Growth and heavy metals removal efficiency of *Nostoc muscorum* and *Anabaena subcylindrica* in sewage and industrial wastewater effluents. Environ. Toxicol. Pharmacol. **19:**357–365.
15. **Gaither, L. A., and D. J. Eide.** 2001. Eukaryotic zinc transporters and their regulation. Biometals **14:**251–270.
16. **Gardea-Torresdeya, J. L., J. L. Arenasb, N. M. C. Franciscob, K. J. Tiemanna, and R. Webbb.** 1998. Ability of immobilized cyanobacteria to remove metal ions from solution and demonstration of the presence of metallothionein genes in various strains. J. Hazardous Substance Res. **1:**2–18.
17. **Gaur, J. P., and L. C. Rai.** 2001. Heavy metal tolerance in algae in algal adaptation to environmental stresses: physiological biochemical and molecular mechanisms, p. 363–388. Springer-Verlag, Heidelberg, Germany.
18. **Grass, G., M. D. Wong, B. P. Rosen, R. L. Smith, and C. Rensing.** 2002. ZupT is a Zn(II) uptake system in *Escherichia coli*. J. Bacteriol. **184:**864–866.
19. **Guerinot, M. L.** 2000. The ZIP family of metal transporters. Biochim. Biophys. Acta **1:**190–198.
20. **Guffanti, A. A., Y. Wei, S. V. Rood, and T. A. Krulwich.** 2002. An antiport mechanism for a member of the cation diffusion facilitator family: divalent cations efflux in exchange for K^+ and H^+. Mol. Microbiol. **45:**145–153.
21. **Hantke, K.** 2005. Bacterial zinc uptake and regulators. Curr. Opin. Microbiol. **8:**196–202.
22. **Hantke, K.** 1981. Regulation of ferric iron transport in *Escherichia coli* K12: isolation of a constitutive mutant Mol. Gen. Genet. **182:**288–292.
23. **Higgins, D. G., and P. M. Sharp.** 1988. Clustal: a package for performing multiple sequence alignment on microcomputer. Gene **73:**273–274.
24. **Incharoensakdi, A., and P. Kitjaharn.** 2002. Zinc biosorption from aqueous solution by a halotolerant cyanobacterium *Aphanothece halophytica*. Curr. Microbiol. **45:**261–264.
25. **Krogh, A., B. Larsson, G. von Heijne, and E. L. L. Sonnhammer.** 2001. Predicting transmembrane protein topology with a hidden Markov model: application to complete genomes. J. Mol. Biol. **305:**567–580.
26. **Lee, J. W., and J. D. Helmann.** 2007. Functional specialization within the Fur family of metalloregulators. Biometals **20:**485–499.
27. **Liu, T., S. Nakashima, K. Hirose, M. Shibasaka, M. Katsuhara, B. Ezaki, D. P. Giedroc, and K. Kasamo.** 2004. A novel cyanobacterial SmtB/ArsR family repressor regulates the expression of a CPx-ATPase and a metallothionein in response to both Cu(I)/Ag(I) and Zn(II)/Cd(II). J. Biol. Chem. **279:**17810–17818.
28. **Meeks, J. C., J. Elhai, T. Thiel, M. Potts, F. Larimer, J. Lamerdin, P. Predki, and R. Atlas.** 2001. An overview of the genome of *Nostoc punctiforme*, a multicellular, symbiotic cyanobacterium. Photosynth. Res. **70:**85–106.
29. **Mehta, S. K., and J. P. Gaur.** 2005. Use of algae for removing heavy metal ions from wastewater: progress and prospects. Crit. Rev. Biotechnol. **25:**113–152.
30. **Mills, S. A., and M. A. Marletta.** 2005. Metal binding characteristics and role of iron oxidation in the ferric uptake regulator from *Escherichia coli*. Biochemistry **44:**13553–13559.
31. **Nies, D. H.** 2003. Efflux-mediated heavy metal resistance in prokaryotes. FEMS Microbiol. Rev. **27:**313–339.
32. **Nies, D. H.** 1992. Resistance to cadmium, cobalt, zinc, and nickel in microbes. Plasmid **27:**17–28.
33. **Palmiter, R. D., and L. Huang.** 2004. Efflux and compartmentalization of zinc by members of the slc30 family of solute carriers. J. Physiol. **447:**744–751.
34. **Parker, D. L., L. C. Rai, N. Mallick, P. K. Rai, and H. D. Kumar.** 1998. Effects of cellular metabolism and viability on metal ion accumulation by cultured biomass from a bloom of the cyanobacterium *Microcystis aeruginosa*. Appl. Environ. Microbiol. **64:**1545–1547.
35. **Patzer, S. I., and K. Hantke.** 1998. The ZnuABC high-affinity zinc uptake system and its regulator Zur in *Escherichia coli*. Mol. Microbiol. **28:**1199–1210.
36. **Paulsen, I. T., and M. H. Saier.** 1997. A novel family of ubiquitous heavy metal ion transport proteins J. Membr. Biol. **156:**99–103.
37. **Pedone, E., S. Bartolucci, and G. Fiorentino.** 2004. Sensing and adapting to environmental stress: the archaeal tactic. Front. Biosci. **9:**2909–2926.
38. **Pohl, E., J. C. Haller, A. Mijovilovich, W. Meyer-Klaucke, E. Garman, and M. L. Vasil.** 2003. Architecture of a protein central to iron homeostasis: crystal structure and spectroscopic analysis of the ferric uptake regulator Mol. Microbiol. **47:**903–915.
39. **Pradhan, S. P., J. R. Conrad, J. R. Paterek, and V. J. Srivastava.** 1998. Potential of phytoremediation for treatment of PAHs in soil at MGP sites. Soil Sediment Contam. **7:**467–480.
40. **Qiu, A., and C. Hogstrand.** 2005. Functional expression of a low-affinity zinc uptake transporter (Fr ZIP2) from pufferfish (*Takifugu rubripes*) in MDCK cells. Biochem. J. **390:**777–786.
41. **Ran, L., F. Huang, M. Ekman, J. Klint, and B. Bergman.** 2007. Proteomic analyses of the photoauto- and diazotrophically grown cyanobacterium *Nostoc* sp. PCC 73102. Microbiology **153:**608–618.
42. **Shin, J. H., S. Y. Oh, S. J. Kim, and J. H. Roe.** 2007. The zinc-responsive regulator Zur controls a zinc uptake system and some ribosomal proteins in *Streptomyces coelicolor* A3(2). J. Bacteriol. **189:**4070–4077.
43. **Thompson, J. D., T. J. Gibson, F. Plewniak, and D. G. Higgins.** 1997. The CLUSTAL X Windows interface: flexible strategies for multiple sequence alignment aided by quality analysis tools. Nucleic Acids Res. **25:**4876–4881.
44. **Thompson, J. D., D. G. Higgins, and T. J. Gibson.** 1994. CLUSTAL W: Improving the sensitivity of progressive multiple sequence alignment through sequence weighting position-specific gap penalties and weight matrix choice Nucleic Acids Res. **22:**4673–4680.
45. **Vannela, R., and S. K. Verma.** 2006. Co^{2+}, Cu^{2+}, and Zn^{2+} accumulation by cyanobacterium *Spirulina platensis*. Biotechnol. Prog. **22:**1282–1293.
46. **Vidali, M.** 2001. Bioremediation: an overview. Pure Applied Chem. **73:**1163–1172.
47. **Wilson, D., G. Varigos, and M. L. Ackland.** 2006. Apoptosis may underlie the pathology of zinc-deficient skin. Immunol. Cell Biol. **84:**28–37.
48. **Yamamoto, K., and A. Ishihama.** 2005. Transcriptional response of *Escherichia coli* to external zinc. J. Bacteriol. **187:**6333–6340.